

Why study pulsars optically?

A. Shearer¹, A. Golden¹

Computational Astrophysical Laboratory, National University of Ireland, Galway, Ireland

Abstract. Observations of the five confirmed optical pulsars indicate that the peak emission scales according to the magnetic field strength at the light cylinder. To the accuracy that such low number allows we show that this gives further confirmation that a straightforward synchrotron model such as Pacini & Salvati (1987) still has validity. The derived relationships indicates that the emission mechanism is common across all of the pulsars and towards the edge of the light cylinder. In the future observations should include near and far infra red work to determine the long wave self absorption cut-off and polarization observations of all pulsars to restrict (to first order) emission zone geometry

terms of its simplicity and longevity) has been proposed by Pacini (1971) and in modified form by Pacini and Salvati (1983; PS83, 1987; PS87). In general the model proposed that the high energy emission comes from relativistic electrons radiating via synchrotron processes in the outer regions of the magnetosphere, and that the location and approximate dimensions of this emission region scales with the magnetic field in the vicinity of the light cylinder. In this paper we examine the validity of their approach and show that it adequately explains the observed phenomena.

In recent years a number of groups have carried out detailed simulations of the various high-energy emission processes. These models divide into two broad groups - between acceleration and emission low in the magnetosphere (Polar Cap models Daugherty & Harding (1996)) and those with the acceleration nearer to the light cylinder (Outer-Gap models Cheng et al (2000) and refs therein). Both models have problems explaining the observed features of the limited selection of high energy emitters. However both models suffer from arbitrary assumptions in terms of the sustainability of the outer-gap and the orientation of the pulsar’s magnetic field to both the observers line of sight and the rotation axis. Furthermore some observational evidence, see for example Eikenberry & Fazio (1997), severely limits the applicability of the outer-gap to the emission from the Crab pulsar. However they have their successes - the total polar-cap emission can be understood in terms of the Goldreich and Julian current from in or around the cap; the Crab polarization sweep is accurately produced by an outer-gap variant Romani & Yadigaroglu (1995). Until we have more detailed observations - and in the optical all aspects of the radiation can be measured (intensity, timing, energy and polarization) - on more objects the situation will not improve.

It is the failure of the detailed models to explain the high energy emission that has prompted this work. We have taken a phenomenological approach to test whether Pacini type scaling is still applicable. Our approach has been to try and restrict the effects of geometry by taking the peak luminosity as a scaling parameter rather than the

1. Introduction

Since the first optical observations of the Crab pulsar in the late 1960s (Cocke et al (1969) only four more pulsars have been seen to pulsate optically (PSR B0540-69; Middleditch & Pennypacker(1985); Vela: Wallace et al (1977); B0656+14; Shearer et al (1997); Geminga; Shearer et al (1998)). Four of these five pulsars are probably too distant to have any detectable optical thermal emission using currently available technologies. For the fifth (and faintest) pulsar, PSR 0633+17, spectroscopic studies have shown the emission to be predominantly non-thermal (Martin et al (1998)). With these objects we are therefore seeing non-thermal emission, presumably from interactions between the pulsar’s magnetic field and a stream of charged particles from the neutron star’s surface. Many suggestions have been made concerning the optical emission process for these young and middle-aged pulsars. Despite many years of detailed theoretical studies and more recently limited numerical simulations, no convincing models have been derived which explain all of the high energy properties. There are similar problems in the radio but as the emission mechanism is radically different (being coherent) only the high energy emission will be considered here. However, the most successful analytical model (both in

Table 1. Observed fluxes from the observed optical pulsars in B and scaled to the VLT. Note the sky background is of the order 1300 photons/sec/arcsec² for the VLT.

Name	Int. Flux (m_B)	Int. Flux ph/sec/VLT
Crab	17	90,000
PSR 0540-69	23	370
Vela	24	150
Geminga	25.5	37
PSR 0656+14	26	23
(PSR 1509-58)	25.7	30)

total luminosity. In this regard we are removing the duty cycle term from PS87. It is our opinion that to first order the peak emission represents the local power density along the observer’s line of site and hence reflects more accurately the emission process within the pulsar’s magnetosphere. Previous work in this area (see for example Goldoni et al (1995)) looked at the total efficiency, spectral index and found no reasonable correlation with standard pulsar parameters - age, period and spin down rate. Their work was hampered by not including geometry and being restricted to the then three known pulsed emitters. Since then the number of optical pulsars has increased to five. However we are still dealing with very weak statistics in all cases bar that of the Crab pulsar.

2. Current Observations - An Overview

2.1. Introduction

The three brightest pulsars (Crab, Vela and PSR B0540-69) are also amongst the youngest. Tables 1 and 2 show the current observed limitations of optical pulsars. Only the Crab is sufficiently bright for individual pulse work to be performed. For the faintest objects very high throughput instruments (including polarimetry) are needed to do more than simple photometry.

Table 4 shows the basic parameters for these objects. However all these pulsars have very different pulse shapes resulting in a very different ratio between the integrated flux and the peak flux. Table 4 also shows this peak emission (taken as the emission in 95% - 95% portion of the largest peak). Their distances imply that the thermal emission should be low (in all cases < 1% of the observed emission). One observational note the Crab is by far the brightest optical by a factor of 250:1. Only the Crab is bright enough for individual pulse work - of all Stokes’ parameters. Furthermore it is the only one for which Stokes’ parameters can be accurately measured throughout the pulsar’s rotation period.

2.2. The Gold Standard - the Crab pulsar

The Crab pulsar’s phase plot is well known - see Figure 1 for R/I (6000-8500 Å) measurements taken with an

Table 2. Observed fluxes from the observed thermally emitting pulsars in B and scaled to the VLT. Note the sky background is of the order 1300 photons/sec/arcsec² for the VLT.

Name	Int. Flux (m_B)	Int. Flux ph/sec/VLT
PSR 1929+10	>26.2	<20
PSR 0950+08	27.2	7
RXJ 1856.5-37.54	25.5	36
PSR 0656+14	>26.8	<14
Geminga	>27	<10
PSR B1055-52	24.9 (U)	≈50

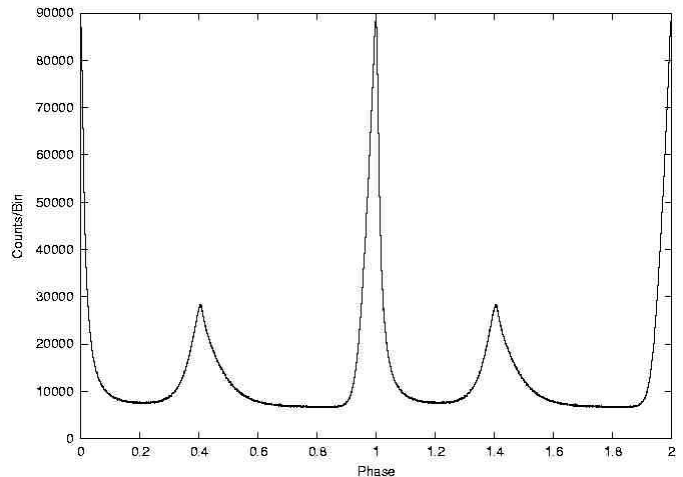


Fig. 1. Crab pulse profile in R and I with 3000 phase bins taken in November 1999 using an APD in the TRIFFID photometer

avalanche photo-diode (APD) on the WHT over 3 nights of observation. Figure 2 shows the peak region indicating the very small plateau. Figure 3 shows 2-d time resolved V band MAMA data - in particular we note emission during the ‘off pulse’ region (phase 0.77-0.84). This is discussed in more detail below.

Over the last thirty years the Crab pulsar has been studied more extensively than any other. It is unique in that its age is known accurately, it is relatively close and bright. One of the main predictions of Pacini (1971) was the prediction that the Crab luminosity should reduce by ≈ 0.005 mags/year. Nasuti et al (1996)’s estimate of 0.008 ± 0.004 / year is in agreement with this (see Figure 4). However more detailed observations are required - preferably with the same telescope, detector and filter arrangements to conform this and remove systematic errors.

Smith et al. (1988) made detailed 1-d optical measurements of the phase resolved polarization, displayed in Figures 6 & 7. They noted that the polarization percentage followed the same shape over the main and interpulse. However interestingly they noted that the highest level of polarization was evident in the ‘off’-pulse region. Smith et al (1988) went to some considerable lengths to

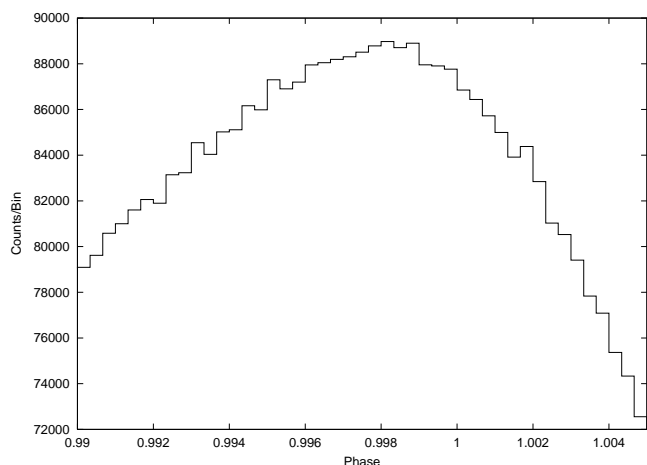


Fig. 2. The peak of the Crab pulse (from the same data set as Figure 1 showing the small or non-existent plateau

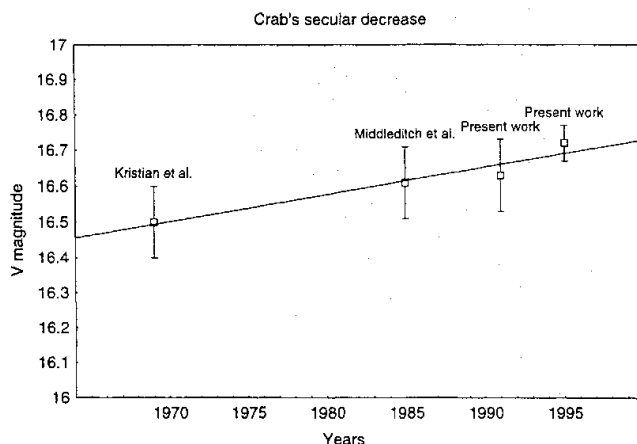


Fig. 4. Secular change on Crab luminosity - from Nasuti et al (1996)

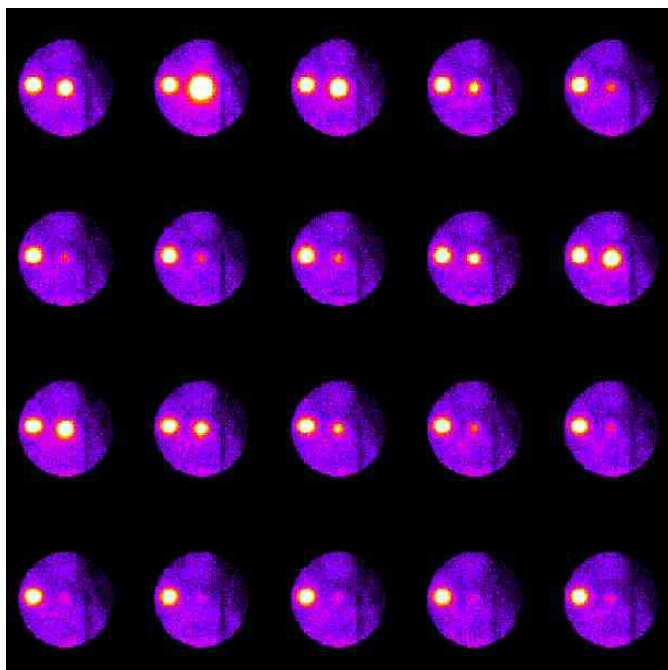


Fig. 3. Phase resolved images taken over three nights using a 2-d MAMA camera in B on the Russian 6m telescope.

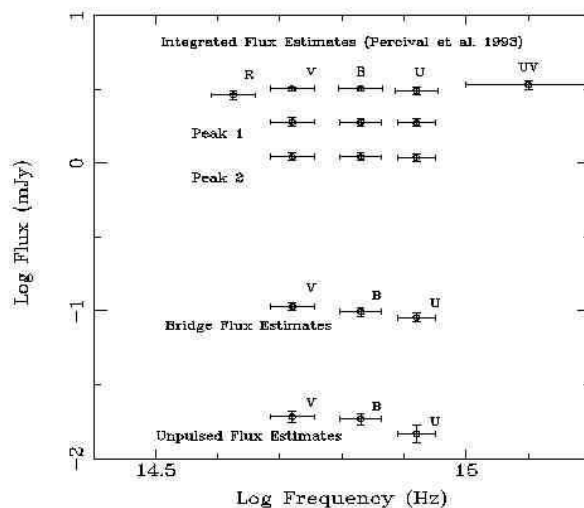


Fig. 5. *UBV* spectrophotometry of the Crab pulsar's light curve components Golden et al (2000)

remove the background nebular polarization component, and thus viewed this latter result as a consequence of the 'unpulsed' component being a cusp region between the two pulses. They also noted that the polarization angle swings in similar way through the main and interpulse which they interpreted as indicating a similar source (and geometry) of the radiation for both pulses, but coming from opposite poles. A similar, albeit slightly phase shifted, result has been observed by Romani et al (2001) using the new Transition Edge Detector (see Figure 18).

The Crab's spectrum shows no evidence for a low energy break (see for example Sollerman & Flyckt (2002)

and references therein) towards the IR regime, rather some suggestion of a 'levelling' of the spectral index (see Figure 8). Thus far no other optical pulsar has been seen to show evidence for a spectral break at low energies, although we are to some extent constrained by their faintness and the limitations of current high speed detector technology in this waveband. A definitive measurement of the Crab suggested 'roll-over' - indicative of some form of optically thick transition such as self-absorption - in the IR is one of the remaining crucial measurements which should be performed in the next few years.

An unpulsed optical component of emission has been noted for some time, since the work of Peterson et al (1978), although accurate high speed 2-d photometry as always dogged previous efforts to flux the apparent emission. Golden et al (2000) using a MAMA based system obtained sufficient S/N and

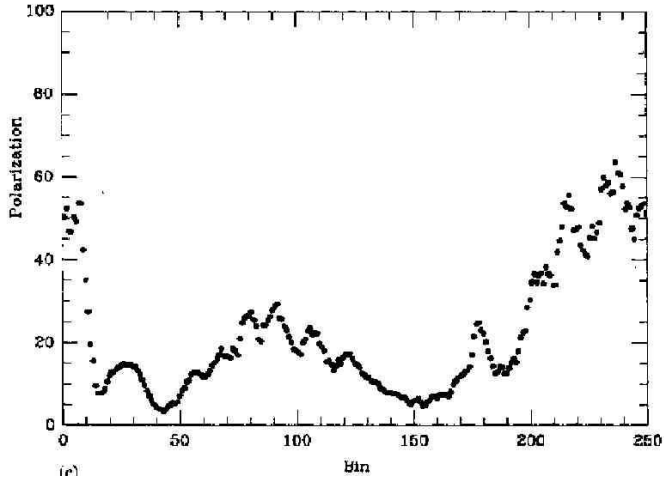


Fig. 6. Crab polarization profile from Smith et al 1988

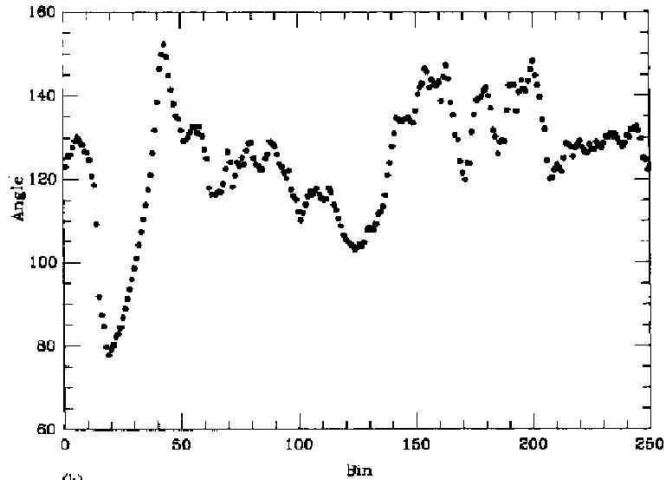


Fig. 7. Crab polarization angle from Smith et al 1988

critically, excellent background statistics to allow for an accurate determination of the flux of this component - clearly apparent in Figure 3, and broad-band spectra in UVB in Figure 5. This unpulsed region, described by Golden et al (2000), can be interpreted in two ways - either a chance alignment of (e.g. a knot) or as a near constant background component to the emission. The star like point source unpulsed image in Figure 3 showed no significant positional shift compared to the integrated position - a shift of at least 3 pixels would be expected if was associated with the red knot ($0''.65$ from the pulsar) (see Hester et al (1995) and Sollerman & Flyckt (2002)). Furthermore the intensity of the knot given by Sollerman & Flyckt (2002), does not explain the R/I background level shown in Figure 10.

2.3. The Remaining Optical Pulsars

Table 1 gives a summary of the observational data of the 5 pulsars seen to give pulsed magnetospheric emis-

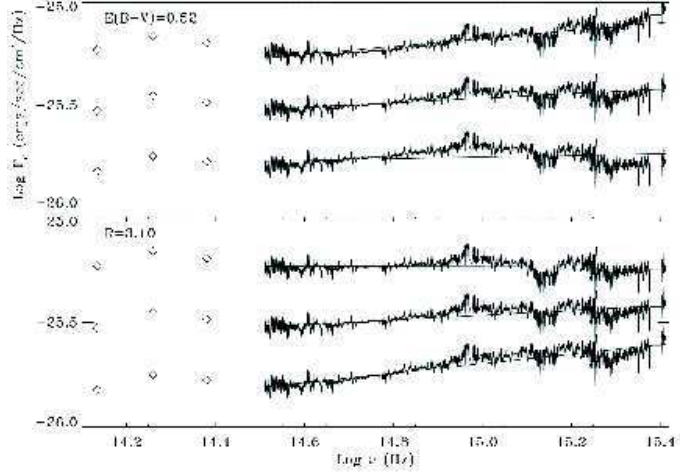


Fig. 8. Crab pulsar spectrum Sollerman et al (2000) with differing values of $E(B-V)$ and R . For $E(B-V) = 0.52$, fits are [$R = 2.9$ (top), 3.1 & 3.3], for $R = 3.1$, fits are [$E(B-V) = 0.49$ (top), 0.52 & 0.55]. Spectra have been shifted by -0.3 , 0.0 & $+0.3$ dex in ‘flux’ for clarity. Eikenberry & Fazio (1997) JHK data are included - these are consistent with 2MASS photometry for the pulsar.

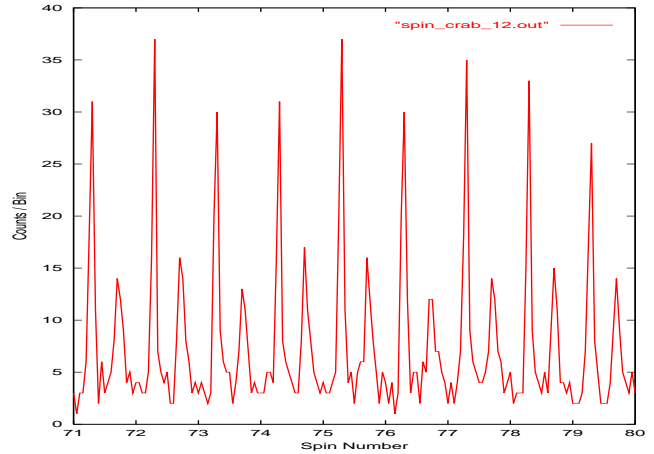


Fig. 9. Individual Crab pulses - statistical analysis shows no deviation from the expectation of Poissonian statistics. There is no observed correlation with the radio giant pulses Shearer et al (2002b)

sion. Of all the optical pulsars PSR B0633+17 (or Geminga) is perhaps the most controversial. Early observations (Halpern & Tytler (1988); Bignami et al (1988)) indicated that Geminga was an ≈ 25.5 mV object. Subsequent observations including HST photometry appeared to support a thermal origin for the optical emission combined with a cyclotron resonance feature (Mignani et al (1998)). The high-speed optical observations of Shearer et al (1998) combined with spectroscopic observations (Martin et al (1998)) contradict this view. Figure 11 shows the broadband data plotted on top of the Martin et al Keck spectra, we have also included

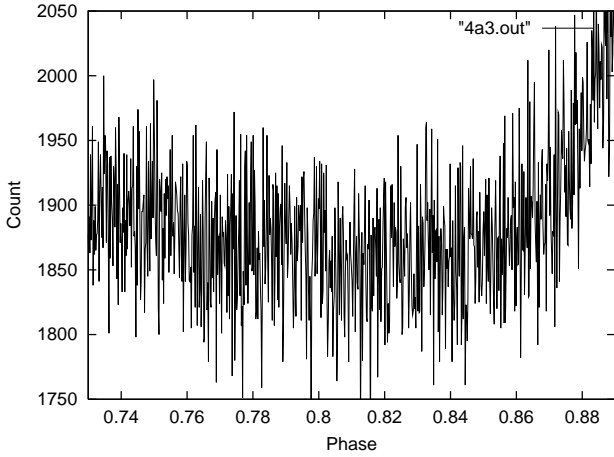


Fig. 10. 'Off' pulse region of Crab pulsar - taken from the full pulse in figure 1. The sky background in this image is at 4390 counts. The knot, see for example Sollerman et al (2000) & Sollerman & Flyckt (2002), situated $0''.6$ from the pulsar (and within our aperture) would contribute a further 650 counts/bin

the pulsed B point acquired via a ground-based MAMA system (Shearer et al (1998)) and recent Subaru data (Kawai et al (2002)). This combined dataset indicates a fairly steep spectrum (with spectral index of ~ 1.9) consistent with magnetospheric emission. It was on the basis of these results that Golden & Shearer (1999) were able to give an upper limit of R_∞ of about 10km by considering the upper limits to the unpulsed fraction of the optical emission from Geminga as an upper limit for the thermal emission. The evolving picture for Geminga is that the soft X-ray and EUV data is predominantly thermal with a magnetospheric component becoming dominant at about 3500 \AA .

As regards PSR B0656+14, the pulsar is generally agreed to be predominantly a non-thermal emitter in the optical, becoming a thermal emitter at wavelengths shorter than about 3000 \AA (Pavlov et al (1997)). There is a discrepancy between the radio distance based upon the dispersion measure and the best fits to the X-ray data. From radio dispersion measure a distance of $760 \pm 190 pc$ can be derived at odds with the X-ray distance of $250 - 280 pc$ from N_H galactic models. A similar low estimate for the distance was given by Kaplan et al (2001). The optical spectrum is best fitted by a two component model with the power law component being significantly steeper than the Crab. Both Geminga and PSR B0656+14 have steep spectra compared their younger cousins. The observed light curve is roughly sinusoidal presumably indicative of closer alignment between the observer and the rotation axis than for the Crab and Geminga.

PSR B0540-69, the second brightest optical pulsar, is also the most distant. It is regarded as a twin of the Crab

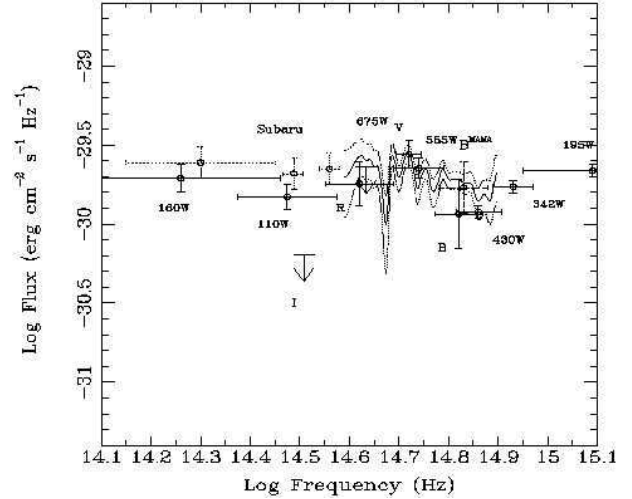


Fig. 11. Spectra and Photometry of Geminga. The spectrum (Martin et al (1998)) and the agreement between it and the integrated photometry (Mignani et al (1998)). B is the pulsed flux from Shearer et al (1998). The HST points are from Pavlov, private communication - these are in close agreement with the IR points presented at this workshop Kawai et al (2002).

as it is of similar age, spin-down energy, braking index and it is embedded within its own plerionic remnant. It has a broad light-curve with two distinct peaks - see figure 12. The difference between its light curve and that of the Crab is likely due to geometry. This pulsar has also had its braking index measured, $n = 2.2 \pm 0.02$ (Boyd et al (1995)). This (like the Crab) differs from the pure dipole value of 3. Middleditch et al (1987) measured no residual polarization from this pulsar - albeit at low significance.

The Vela pulsar has not been studied extensively in the optical. The best light curve from Gouiffes & Ogelman (1996) shows strong similarity between the γ -ray profile and the optical. More data is required to establish both the detailed structure of the light curve and the pulsar's polarization properties.

2.4. Discussion

In Table 1 we have indicated the peak flux normalized to the Crab pulsar. When comparing the individual pulsars (which will have a range of viewing angles and differing magnetic/rotation axes), we have to account for the viewing angle (related to the pulse duty cycle and separation in terms of phase) as well as the total flux. Furthermore for each source, we have to account for the shape of the pulsar's spectrum. PS87 indicates for emission above the low energy cut-off that the ratio of the fluxes from two different pulsars can be given by Equation 1 if one ignores the effect of duty cycle and pitch angle (the suffixes refer to each pulsar). Here $F_{\nu,n}$ refers to the flux at the observed frequency ν for pulsar n (similarly

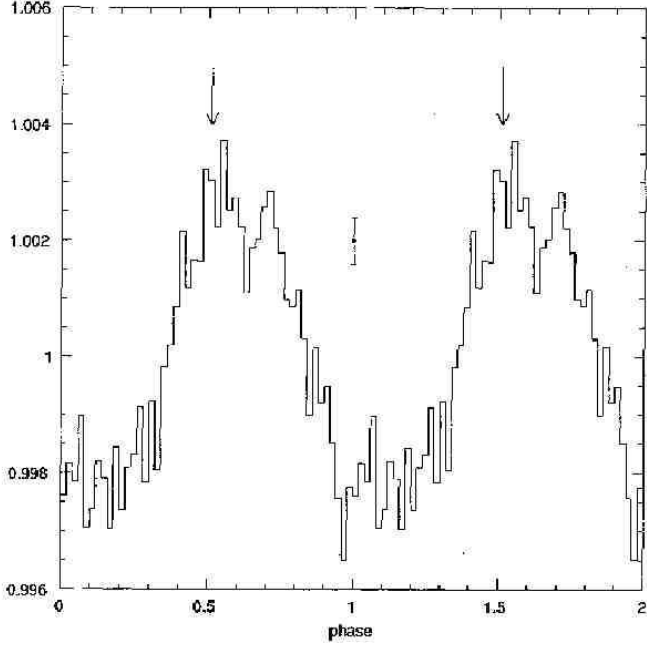


Fig. 12. Light Curve of PSR B0545-69 from Gouiffes et al (1992)

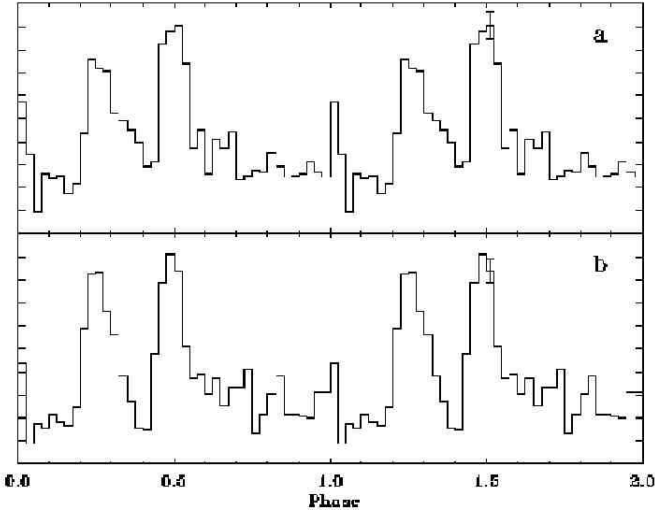


Fig. 13. Vela light curve from Gouiffes & Ogelman (1996)

for the magnetic field strength, B , and period, P). The observed energy spectrum exponent is given by α_n . The duty cycle can be accounted for by only considering the peak emission. The pitch angle being beyond the scope of this work and assumed to first order to be invariant. Equation 2 shows the same formulation for the outer field case.

$$\frac{F_{\nu,2}}{F_{\nu,1}} \propto \left(\frac{\nu_{1,0}}{\nu}\right)^{\alpha_2 - \alpha_1} \left(\frac{B_{2,0}}{B_{1,0}}\right)^{4 - \alpha_2} \left(\frac{P_2}{P_1}\right)^{3\alpha - 9} \quad (1)$$

Scaling to the transverse field would give:

$$\frac{F_{\nu,2}}{F_{\nu,1}} \propto \left(\frac{\nu_{1,0}}{\nu}\right)^{\alpha_2 - \alpha_1} \left(\frac{B_{2,0}}{B_{1,0}}\right)^{4 - \alpha_2} \left(\frac{P_2}{P_1}\right)^3 \quad (2)$$

Given the observed peak luminosities we investigated the correlation between the peak emission and the surface field and the tangential light cylinder field. Figure 14 shows the relationship between the peak luminosity with the outer (tangentially at the light cylinder) magnetic field strength, B_T , Goldreich-Julian current and canonical age $\left(\frac{P}{2P}\right)$. A clear correlation is seen with all these parameters. We are interested in investigating the implications of a correlation between the peak luminosity and the transverse field. We accept the the strong correlation with G-J current would under pin both emission from polar as well as outer regions.

A regression of the form:

$$\text{Peak Luminosity} \propto B_T^\beta$$

was performed for the empirical peak luminosity this leading to a relationship of the form :-

$$\text{Peak Luminosity} \propto B_T^{2.86 \pm 0.12}$$

significant at the 99.5% level and consistent with the high average exponent shown in Table 1. Figure 14 shows the predicted peak luminosity from Equation 2 against our observed peaks accounting for the differing observed energy spectrum exponent at 4500 Å. The slope is 0.95 ± 0.04 and significant at the 99 % level. Whilst informative it still goes no further than previous attempts to understand the phenomena of optical emission. Importantly, we note that the flattening of the peak luminosity relationship for the older, slower pulsars is consistent with their having a significantly steeper energy spectrum than the younger pulsars, see Table 2. Whilst this is consistent with the emission zone being optically thick we consider it to be more likely that it reflects a larger emission region for these pulsars rather than the younger ones. This broadly concurs with PS87 argument of Δ (the size of the emission zone) scaling with P .

The polarization of the Crab's 'off-region' can be interpreted as coming from a different source to the main pulsed emission. Smith et al's argument that the off emission represented a cusp between the two main pulses relies upon the 'off'-pulse being a genuine cusp and not flat as observed by Shearer et al (2002a). The flat region - see Figure 10 - covers the peak of polarization noted by Smith et al. Another explanation is that the net polarization is a combination of two components; the remnants of a pulsed 'normal' magnetospheric component and a secondary unpulsed 'off-pulse' component. The derived polarization profile is then just the intensity normalized combination of these two processes. As the bridge component has twice the intensity of the 'off'-pulse we would

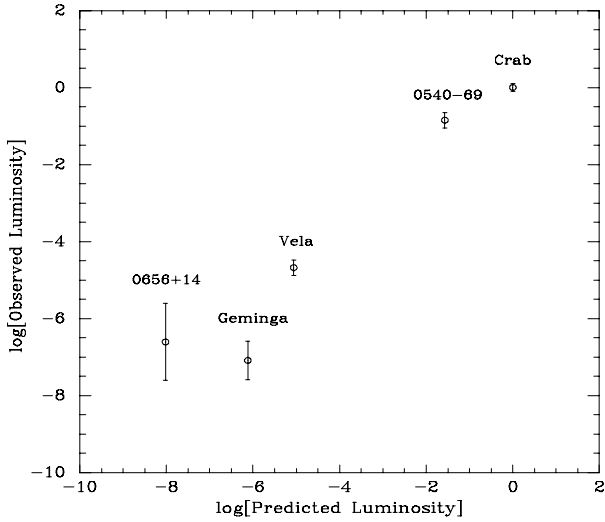


Fig. 14. Observed Peak optical luminosity vs predicted

expect the degree of polarization to be half that of the off-pulse region - as observed. The swing in polarization can therefore be understood in terms of the unpulsed component becoming dominated by the pulsed component during the rising edge of each pulse. The relative contributions being due to normal quadratic addition of the Stokes parameters - i.e. dominated by the relative intensity. Figure 17 shows the derived polarization profile if it only comes from a steady low-level background source. The shape agrees well with the previously measured profile from Smith et al, except in the region around the main and inter-pulse - where the main pulsed polarization component will occur.

It seems clear that from both polarization studies (Smith et al (1988); Romani & Yadigaroglu (1995)) and from this work that we expect that optical emission zone is sited towards the outer magnetosphere. Timing studies of the size of the Crab pulse plateau indicates a restricted emission volume (≈ 45 kms in lateral extent) (Golden et al (2000)). This third point, if consistent with the first two, probably points to emission coming from a geometrically defined cusp along our line of sight akin to treatment within the magnetosphere. More importantly the simple relationships we have derived here indicate that there is no need to invoke complex models for this high energy emission. Observed variations in spectral index, pulse shape and polarization can be understood in terms of geometrical factors rather differences in the production mechanism.

We note as well as that similar trends can be seen in γ rays. Figure 16 shows the correlation between the peak γ emission as a function of transverse field. This indicates a regression of the form

$$\text{Peak } \gamma \text{ Luminosity} \propto B_T^{0.89 \pm 0.15}$$

significant at the 99.6 % level, consistent with the observed steeper distribution seen in the high energy γ -ray band (cf. Table 2).

If we take our results and those of Goldoni et al (1995) we can begin to understand how the high energy emission process evolves with canonically derived pulsar age. Goldoni et al compared the known spectral indices and efficiencies in both the optical and γ -ray regions. They noted that the spectral index flattened with age for the γ -ray pulsars whilst the reverse was true for the optically emitting systems. They also noted a similar trend reversal for the efficiency with the γ -ray pulsars becoming more efficient with age. We note (see the bottom panel in Figures 15 and 16) a similar behaviour with the peak emission. If, as seems likely from the temporal coincidence between the γ -ray and optical pulses, that the source location is similar for both mechanisms. One explanation is that we seem to have a position where by from the same electron population there are two emission processes - expected if we have curvature for the γ -ray photons and synchrotron for the optical ones. It seems likely that the optical photon spectrum has been further modified to produce the reversal in spectral index with age. The region over which the scattering can occur would scale with the size of the magnetosphere and hence with age. With the outer magnetosphere magnetic fields for these pulsars being $< 10^6$ G electron cyclotron scattering is not an option. However synchrotron self-absorption could explain the observed features. In essence we would expect the most marked flattening to be for the Crab pulsar where the outer field strengths are of order 10^6 G and less so for the slower and older systems.

These results (both optical and γ rays) are consistent with a model where the γ and optical emission is coming from the last open-field line at some constant fraction of the light cylinder. The drop in efficiency with age for the production of optical photons points towards an absorbing process in the outer magnetosphere. Clearly more optical and γ -ray observations are needed to confirm these trends.

3. Instrumental Considerations

Table 3 summarizes the current range of detectors available for studies of optical pulsars. To obtain the necessary background measurements 2-d imaging detectors are required - these however (e.g. the MAMA detector used in the TRIFFID photometer, Butler et al (1998)) have limited quantum efficiency. However the limited qe can be offset by reduced effective sky aperture - the TRIFFID photometer uses off-line sky apertures determined by the local seeing conditions.

CCD based detectors, e.g. ULTRACAM (Dhillon & Marsh (2001)), suffer from read-noise problems - which increase with decreasing period/time resolution. These will be effective for AXP studies but 'conventional' pulsars have too short a period. Tech-

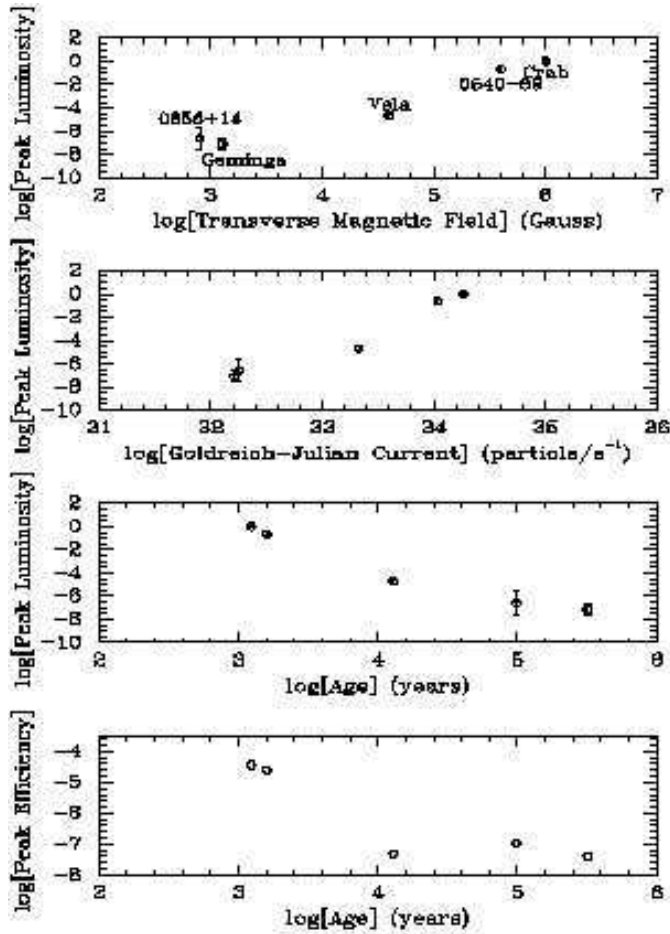


Fig. 15. Peak optical luminosity vs Light Cylinder magnetic field strength, GJ Current and age. Also shown is the optical efficiency as a function of age.

Table 3. Current detector possibilities. The future should lie with the energy sensitive detectors once the number of pixels can be increased

Detector	Time Resolution	Quantum Efficiency	Number of Pixels
CCDs	10 secs +	70%	millions
Fast CCDs e.g. UltraCam	100ms+	70%	millions
APDs			
Optima	μ secs +	70%	single
TRIFFID	μ secs +	70%	single
Photocathode based systems			
2-d - (e.g.) MAMA	μ secs +	<10%	million
Photomultipliers	nsecs +	30% max	single
Energy Sensitive Detectors			
TES	nsecs +	70% max	few
STJ (SCAM)	nsecs +	70%max	few

niques such as on-chip phase locked image shifting and

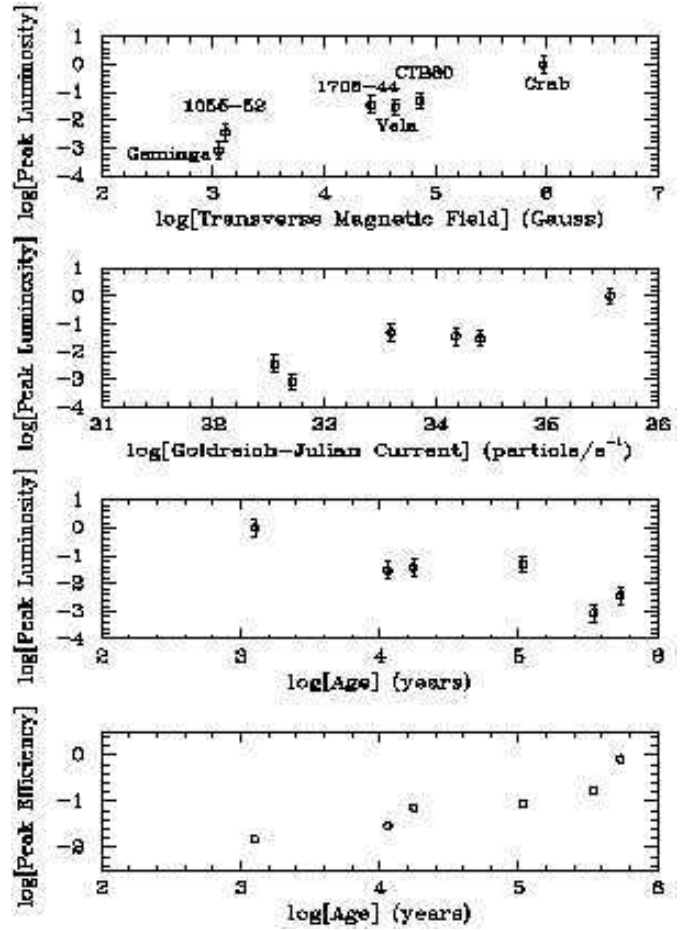


Fig. 16. Outer field strength against peak γ ray luminosity. The γ ray peak luminosity has been inferred from Fierro et al (1998), Thompson et al (1996), Thompson et al (1999)

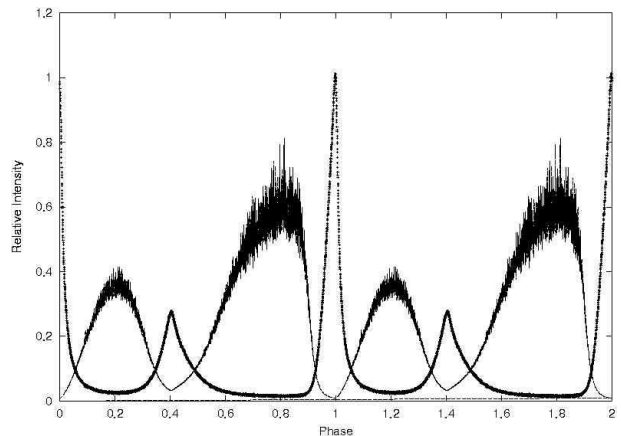


Fig. 17. Crab light curve and inferred polarization fraction using Stokes parameters (Q/U) given by Smith et al (1988) for the off pulse region and then scaled. The contribution from the main pulsar component is not shown.

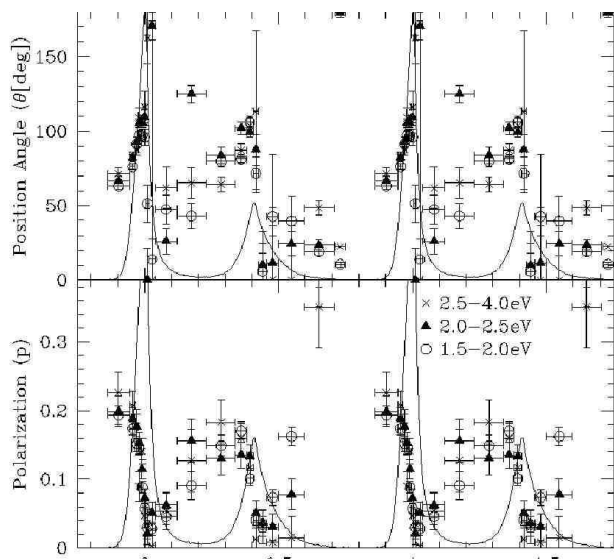


Fig. 18. Crab polarization as a function of pulsar phase measured using the energy sensitive TES from Romani et al (2001)

phase locked moving the secondary mirror have limited application due to field crowding.

Avalanche Photodiodes - as used in OPTIMA (Straubmeier et al (2001)) and TRIFFID - have good quantum efficiency, timing, but, are only single pixel devices. In both Optima and TRIFFID more than one APD is used for different colours and sky background determination. Attempts are currently being made to construct arrays of these items but there are serious cross-talk problems. The next generation of energy sensitive detectors (see for example, Perryman et al (1999) & Romani et al (1999)) will give pulsar observers almost all (with the exception of polarization) flux parameters. However given that these devices are still in their relative infancy there is still a place of APDs and 2-d photocathode based systems.

4. Conclusion

The number of optically emitting pulsar which have been observed is limited. The observed phenomenology points to emission in the outer region of the magnetosphere - this seems more likely to come from an Outer Gap type model rather than a Polar Cap. However the data is sparse and no definitive statement can be made separating these models on the basis of the optical emission alone. Over the next few years as with the advent of larger telescopes and more sensitive detectors, we can confidently expect the number of optical detections of isolated neutron stars to increase. PSR B1055-52 & PSR B1951+32 are likely early candidates.

In the optical any potential thermal component should be separable from the strongly pulsed magnetospheric

emission, allowing for reliable estimates of the neutron star radius to be measured with consequent implications for equation of state models. However before this is done with any degree of confidence the nature of the unpulsed emission must be established - is it a synchrotron knot feature or more localized to the pulsar. Is it unique to the Crab pulsar? Of crucial importance in the future will be determination of the low-energy cutoff and the polarization sweep through the optical pulse (significantly modern instruments are capable of measuring the polarization sweep for both PSR B0540-69 and Vela as well as the Crab). Also of interest will be the shape of the pulse - in particular the size of any plateau which scales as the size of the emission zone. All of these parameters are measurable with existing technologies and telescopes for these pulsars. The advent of new detectors and larger telescopes should herald a period of renewed interest in optical pulsar studies, however there are still important questions that can be answered by observation with existing telescope/instrument systems.

5. Acknowledgments

Enterprise Ireland is acknowledged for support under its Basic Research Grant Scheme. Ray Butler and Padraig O'Connor are thanked for help during the preparation of this manuscript. The workshop organizers are thanked for their hospitality.

References

- Bignami, G. F., Caraveo, P. A. & Paul, J. A., 1988, *A & A*, 202, L1
- Boyd, P. T. et al, 1995, *ApJ*, 448, 365
- Butler, R. F. & Shearer, A. & Redfern, R. M., Colhoun, M., O'Kane, P., Penny, A. J., Morris, P. W., Griffiths, W.K. & Cullum, M., 1998, *MNRAS*, 296, 379
- Cocke, W. J., Disney, M. J. & Taylor, D. J., 1969, *Nature*, 221, 525
- Caraveo, P. A., Bignami, G. F., Mignani, R. & Taff, L. G., 1996, *A & A*, 120, 65
- Cheng, K. S., Ruderman, M. & Zhang, L., 2000, *ApJ*, 537, 964
- Dhillon, V. & Marsh, T, 2001, *NewAR*, 45, 91
- Daugherty, J. K. & Harding, A. K., 1996, *ApJ*, 458, 278
- Eikenberry, S. S. & Fazio, G. G., 1997, *ApJ*, 476, 281
- Fierro, J. M., Michelson, P. F., Nolan, D. C. & Thompson, D. J., 1998, *ApJ*, 494, 734
- Gil, J. A., Khechinashvili & Melikidze, G. I., 2000, to be published in *MNRAS*
- Golden, A. & Shearer, A., 1999, *A & A*, 342, L5
- Golden, A., Shearer, A. & Beskin, G. M., 2000, *ApJ*, 535, 373
- Goldoni, P., Musso, C., Caraveo, P. A. & Bignami, G. F., 1995, *ã*, 298, 535
- Gouiffes, C., Finley, J. P. & Oegelman, H., 1992, *ApJ*, 394, 581
- Gouiffes, C. & Oegelman, H., 1996 *ASP Conf. Ser.* 105: IAU Colloq. 160: Pulsars: Problems and Progress, 299
- Halpern, J-P & Tytler, D., 1988, *ApJ*, 330, 201
- Hester, J. J. et al, 1995, *ApJ*, 448 240

Table 4. Main Characteristics of Optical Pulsars: B_S & B_{LC} the canonical surface and transverse magnetic field at the light cylinder respectively; Opt. Lum and Peak Lum. refer to the optical luminosity at the indicated distance in the B band.

Name	D (kpc)	P (ms)	\dot{P} 10^{-14} s/s	B_S log(G)	B_{LC} log (G)	Int μ Crab	Peak μ Crab	Spectral Index at 4500 Å	Cutoff Å
Crab	2	33	40	12.6	6.1	10^6	10^6	-0.11	>20000
Vela	0.5	89	11	12.5	4.8	27	21	0.2	6500(?)
PSR0545-69	49	50	40	12.7	5.7	$1.1 \cdot 10^6$	$1.4 \cdot 10^5$	0.2	>7000
PSR0656+14	0.76(?)	385	1.2	12.7	3.0	1.8	0.3	1.3	>8000
PSR0633+17	0.16	237	1.2	12.2	3.2	0.3	0.1	1.9	>8000

Table 5. Main Characteristics of γ -ray Pulsars: B_S & B_{LC} the canonical surface and transverse magnetic field at the light cylinder respectively; γ Lum and Peak Lum. refer to the γ luminosity at the indicated distance for $E > \text{MeV}$.

Name	D (kpc)	P (ms)	\dot{P} 10^{-14} s/s	B_S log(G)	B_{LC} log (G)	Int Lumin. Crab=1	Peak Lumin. Crab=1	Spectral Index
Crab	2	33	42.1	12.58	5.97	1	1	2.15
Vela	0.5	89	12.5	12.53	4.64	0.0480	0.0299	1.70
PSR1055-52	49	197	0.6	12.03	3.11	0.0124	0.0037	1.18
PSR1706-44	2.4	102	9.3	12.49	4.42	0.1380	0.0368	1.72
PSR0633+17	0.16	237	1.1	12.21	3.05	0.0019	0.0008	1.50
PSR1951+32	2.5	40	0.6	11.69	4.86	0.0500	0.0187	1.74

Kaplan, D. L., van Kerkwijk, M. H. & Anderson, J., 2001, astro-ph/011174

Kawai et al, 2002, these proceedings

Nasuti, F. P., Mignani, R., Caraveo, P. A. & Bignami, G. F., 1996, A&A, 314, 849

Martin, C, Halpern, J.P. & Schiminovich, D., 1998, ApJ, 494, L211

Middleditch, J. & Pennypacker, C., 1985, Nature, 313, 659

Middleditch, J., Pennypacker, C. & Burns, M. S., 1987, ApJ, 315, 142

Mignani, R. P., Caraveo, P. A., & Bignami, G. F., 1998, Å, 332, L37

Nasuti, F. P., Mignani, R., Caraveo, P. A. & Bignami, G. F., 1996, A&A, 323, 839

Pacini, F., 1971, ApJ, 163,17

Pacini, F. & Salvati, M., 1983, ApJ, 274, 369

Pacini, F. & Salvati, M., 1987, ApJ, 321, 445

Pavlov, G. G., Welty, A. D. & Cordova, F. A., 1997, ApJ, 489, L75

Perryman, M. A. C., Favata, F., Peacock, A., Rando, N. & Taylor, B. G., 1999, A & A, 346, 30

Peterson, B. A., Murdin, P., Wallace, P., Manchester, R. N., Penny, A. J., Jorden, A., Hartley, K. F. & King, D, 1978, Nature, 276, 475

Romani, R. W., & Yadigaroglu, I.-A., 1995, ApJ, 438, 314

Romani, R. W., Millar, A. J., Cabrera, B., Nam, S. W. & Yadigaroglu, I.-A., 2001, astro-ph 0108240

Romani, R. W., Miller, A. J., Cabera, B. & Figueroa-Feliciano, E., 1999, ApJ, 521, L151

Shearer, A., Redfern, R. M., Gorman, G., Butler, Golden, A., R., O’Kane, P., Golden, A., Beskin, G. M., Neizvestny, S. I., Neustroev, V. V., Plokhhotnichenko, V. L. & Cullum, M., ApJ, 1997, 487, L181

Shearer, A., Harfst, S., Redfern, R. M., Butler, R., O’Kane, P., Beskin, G. M., Neizvestny, S. I., Neustroev, V. V., Plokhhotnichenko, V. L. & Cullum, M., 1998, A & A, 335, L21

Shearer, A. & Golden, A., 2001, ApJ, xxx, yyy

Shearer, A., O Connor, P. & Golden, A., Ryan, O., & Redfern, M., in preparation

Shearer, A., Butler, R. F. & Golden, A., in preparation

Smith, F. G., Jones, D. H. P., Dick, J. S. P. & Pike, C. D., 1988, MNRAS, 233, 305

Sollerman, J., Lundqvist, P., Lindler, D., Chevalier, R. A., Fransson, C., Gull, T. R., Pun, C. S. J. & Sonneborn, G, 2000, ApJ, 537, 861

Sollerman, J. & Flyckt, V., 2002, ESO Messenger, 107, 32

Straubmeier, C., Kanbach, G. & Schrey, F., 2001, Exp Ast, 11, 157

Thompson, D. J., 1996, ApJ, 465, 385

Thompson, D. J., 1999, ApJ, 516, 297

Wallace, P. T. et al. 1977, Nature, 266, 692